HHS Public Access

Author manuscript

J Magn Reson Imaging. Author manuscript; available in PMC 2017 November 01.

Published in final edited form as:

J Magn Reson Imaging. 2016 November ; 44(5): 1099–1106. doi:10.1002/jmri.25276.

Applying a New Quantitative Global Breast MRI Feature Analysis Scheme to Assess Tumor Response to Chemotherapy

Faranak Aghaei and **Maxine Tan**

School of Electrical and Computer Engineering, University of Oklahoma, Norman, OK 73019

Alan B. Hollingsworth

Mercy Women's Center, Mercy Health Center, Oklahoma City, OK 73120

Bin Zheng

School of Electrical and Computer Engineering, University of Oklahoma, Norman, OK 73019

Abstract

Purpose—To develop a new quantitative global kinetic breast MRI features analysis scheme and assess its feasibility to assess tumor response to neoadjuvant chemotherapy.

Methods—A dataset involving breast MR images acquired from 151 cancer patients before neoadjuvant chemotherapy was used. Among them, 63 patients had complete response (CR) and 88 had partial response (PR) to chemotherapy based on the RECIST criterion. A computer-aided detection (CAD) scheme was applied to segment breast region depicted on the breast MR images and computed a total of 10 kinetic image features to represent parenchyma enhancement either from the entire two breasts or the bilateral asymmetry between the two breasts. To classify between CR and PR cases, we tested an attribution selected classifier that integrates with an artificial neural network and a Wrapper Subset Evaluator. The classifier was trained and tested using a leave-one-case-out (LOCO) based cross-validation method. The area under a receiver operating characteristic curve (AUC) was computed to assess classifier performance.

Results—From the pool of initial 10 features, 4 features were selected by more than 90% times in the LOCO cross-validation iterations. Among them, 3 represent the bilateral asymmetry of kinetic features between two breasts. Using the classifier yielded AUC = 0.83±0.04, which is significantly higher than using each individual feature to classify between CR and PR cases ($p < 0.05$).

Conclusion—This study demonstrated that quantitative analysis of global kinetic features computed from breast MR images acquired pre-chemotherapy has potential to generate a useful clinical marker that is associated with tumor response to neoadjuvant chemotherapy.

Keywords

Dynamic contrast-enhanced breast magnetic resonance imaging; tumor response to neoadjuvant chemotherapy; quantitative image feature analysis; assessment of breast cancer prognosis; bilateral asymmetry of parenchyma breast MR enhancement

Corresponding Author: Bin Zheng, PhD., School of Electrical and Computer Engineering, University of Oklahoma, Norman, OK 73019, bin.zheng-1@ou.edu.

I. INTRODUCTION

Among the existing imaging modalities of breast cancer detection, diagnosis and prognosis assessment, dynamic contrast enhancement (DCE) breast MRI has superior capability and performance. For example, one review article analyzed 5 prospective clinical studies and revealed a comparison result in which the cancer detection sensitivities were 40% and 81% for mammography and breast MRI, respectively (1). Another large clinical study involving 2,809 women with elevated breast cancer risk also reported that using breast MRI enabled to detect 79% (41/52) mammography-occult cancers (2). Hence, using breast MRI could detect a significantly greater number of cancers than mammography. As a result breast DCE-MRI has been recommended by American Cancer Society as an adjunct screening tool to mammography for women with life time breast cancer risk greater than 20%–25% since 2007 (3). In addition, breast MRI has played an important role in classifying breast tumors (i.e., ductal carcinoma in situ (DCIS) or invasive ductal carcinoma (IDC) with and without metastasis-positive lymph nodes (4)) and evaluate the tumor response to chemotherapy by comparing two sets of breast MR images acquired pre- and post-chemotherapy (5).

In current practice advanced stage breast cancer patients with large breast lesions are treated with neoadjuvant (preoperative) chemotherapy before surgery. Based on the tumor response to the neoadjuvant chemotherapy, a breast cancer patient may receive breast-conserving surgery instead of mastectomy (6–8) or avoid the surgery due to the pathological complete response (pCR) (9, 10), which would improve the life quality of breast cancer patients. Tumor response to the chemotherapy is typically evaluated by comparing tumor size and kinetic feature variation using breast MRI examinations taken pre- and post-chemotherapy based on RECIST guideline (11). However, due to heterogeneity of breast tumors, the response to the neoadjuvant chemotherapy varies widely in different patients (12). Hence, in order to assist clinicians in making an optimal treatment plan for the individual patients early and/or reduce the side effect of the patients who do not receive significant benefit from the neoadjuvant chemotherapy, developing a marker that allows accurate assessment of tumor response may have a high clinical impact. For that purpose, we recently developed and tested a new quantitative kinetic image feature analysis based computer-aided detection (CAD) scheme using breast MR images acquired before the patients participated in the neoadjuvant chemotherapy to assess tumor response to the neoadjuvant chemotherapy (13). From the segmented breast lesions, the scheme computed kinetic image features of the lesions and assess the likelihood of the tumor response to the neoadjuvant chemotherapy using a multi-feature based artificial neural network.

Despite encouraging results in our preliminary study, application of the scheme can be limited or less robust due to the difficulty in accurately defining and/or segmenting the breast lesions, in particular the subtle and/or diffuse lesions without a solid lesion boundary. Recently, the studies reported by several groups (14, 15) demonstrated that the global background parenchyma enhancement (BPE) features extracted from the entire breast MR images can be used to assess breast cancer risk (14) and improve accuracy in classifying between the malignant and benign breast lesions (15). Hence, based on previously published works, the objective of this study is to develop a new quantitatively global kinetic image

feature analysis based CAD scheme without lesion segmentation and test the feasibility of applying this new scheme to assess tumor response to the neoadjuvant chemotherapy.

II. MATERIALS AND METHODS

II.A. A DCE-MRI image dataset

The study protocol including image data collection and data analysis method was approved by our institutional review board. In this retrospectively study, the image data were collected from the existing cases stored in the clinical PACS. The informed consent of the patients were waived. The dataset includes the de-identified breast MR images acquired from 151 breast cancer patients. Each patient had two sets of breast DCE-MRI examinations taken before and after neoadjuvant chemotherapy. The average time difference between two MRI examinations is around 5 months (or 157 days). All MRI examinations were performed using a 1.5 Tesla GE Excite MRI scanner during 2008 and 2010. In each MRI examination, 5 sets of axial images were scanned and acquired. The first one is pre-contrast scan of two breasts. Approximately 3 minutes after intravenous administration of 0.1mmol/kg body weight OptiMARK gadolinium, 4 sets of post-contrast scans started to acquire 4 sets of new axial images. Each image slice has 512 × 512 pixels with a pixel size of 0.6445×0.6445 mm and a slice thickness of 4 mm.

Among the 151 patients, 63 were assigned in complete response (CR) group and 88 were categorized in partial response (PR) group. According to RECIST guidelines, in CR group, the kinetic enhancement signals (or contrast enhanced pixels) inside the tracked breast tumors depicting in the first set of breast MR images acquired pre-chemotherapy become undetectable in the second set of breast MR images acquired post-chemotherapy, while in PR group, the contrast enhanced pixels inside the tumor regions decrease by more than 30% between the post- and pre-chemotherapy breast MR images. Figure 1 shows 3 examples of 2 matched breast MR image slides acquired pre- and post-chemotherapy of 3 patients. In one CR case (Fig. 1(a) and (b)), the contrast enhanced pixels almost disappear inside the target tumor region depicting on the post-chemotherapy breast MR image. In the first PR case (Fig. 1(c) and (d)) a solid tumor has contrast enhanced pixels surrounding tumor boundary and a big necrotic center region. After neoadjuvant chemotherapy, although the tumor diameter was reduced or “partially responsive,” central necrotic region of the tumor also disappears and the active contrast enhancement volume increases after the neoadjuvant chemotherapy. The second PR case (Fig. 1(e) and (f)) shows the lesions with diffused enhancement on breast MR images acquired pre- and post-chemotherapy.

In this dataset, the age of the patients ranged from 25 to 76 years old. The average age and standard deviation are 47.4±11.2 and 49.2±10.4 for CR and PR patient groups, respectively, which indicate that the majority of women whose breast DCE-MRI examination images were selected in this study are relatively younger (< 50 years old). Table 1 summarizes the basic tumor characteristics between the CR and PR case groups. The majority of tumors were diagnosed as invasive ductal carcinoma (IDC) with or without associated DCIS. Finally, the axial view of the breast MR images acquired pre-chemotherapy of each patient was used and analyzed in this study. The goal of this study is using the global kinetic image

features computed from the pre-chemotherapy breast MR images only to build a machine learning classifier or model to assess tumor response to the neoadjuvant chemotherapy.

II.B. Quantitative global kinetic image feature computation

In order to automatically compute global contrast enhancement features, we applied a CAD scheme of breast MR images that has been developed and to segment the breast region depicting on each breast MR image by removing all pixels in the air background and behind the chest wall or pectoralis muscle. The details of this CAD scheme have been reported in our previous publication (13). In brief, the CAD scheme uses the following 4 image processing and feature computation steps namely, (1) applying a threshold method to remove all pixels in the air background of each image, (2) detecting the chest wall depicting on each breast MR image to remove all pixels behind the chest wall (Figure 2); (3) performing image registration and subtraction of two sets of matched breast MR image slices acquired in two breast MRI scans performed pre- and post-injection of gadopentate dimeglumine (Gd-DTPA) contrast agent; and (4) computing a set of relevant kinetic image features from segmented breast region depicted on each subtraction image. By applying this CAD scheme to all breast MR image slides, we are able to yield the global breast contrast enhancement image features of the whole breast volume.

Our CAD scheme initially computed a set of 10 kinetic or contrast enhancement image features from the subtraction images of two sets of registered images acquired pre- and post-injection of contrast agent (as shown in Table 1). Specifically, these features include: *F1* – average contrast enhancement value (EV), which is simply computed as an average of the pixel value of all pixels inside the segmented breast volume, *F2* – standard deviation and *F3* – skewness of the contrast enhancement values, which are two features that measure the heterogeneity of contrast enhancement of the pixel values, *F4* – the maximum contrast enhancement value inside the whole breast volume. In addition, CAD scheme sorted the contrast enhancement values from the maximum to the minimum, which are computed from the whole breast volume, and then computed two new features namely, *F5* – the average contrast enhancement value among the pixels listed in the top 1% and *F6* – in the top 5% of the sorting list. In a previous study, using these two average contrast enhancement values could have higher discriminatory power to assist classifying between malignant and benign breast lesions than using the average or the maximum contrast enhancement value computed from the whole breast regions (16). In addition, CAD scheme also computed four features representing the bilateral differences (or the absolute subtraction) of two feature values computed from the left and right breast regions (*F7* – *F10*).

II.C. Feature analysis and performance assessment

Next, from the initial feature pool of 10 contrast enhancement image features (Table 2), we aimed to select optimal image features and build a machine learning classifier to assess the likelihood of the breast tumors being completely responsible to the neoadjuvant chemotherapy (CR). For this purpose, we used a publicly available data mining and machine learning software platform, Weka (17), to perform feature selection and classifier training and testing tasks. The similar optimization process has been applied and tested in our previous study (13). In brief, we used a specific machine learning classifier namely, the

"AttributeSelectedClassifier", which integrates an artificial neural network (ANN) as the base classifier and a Wrapper Subset Evaluator (WSE) to guide feature selection from the initial pool of 10 features. This integration takes a search algorithm and evaluator next to the base classifier, which makes the feature selection process transparent and the base classifier operates only in a reduced optimal feature space (18).

Due to the limited dataset size of 151 cases, the classifier was trained using a leave-one-case-out (LOCO) method to maximally use all available training cases and also minimize the testing bias (19). In addition, to avoid the bias in feature selection, the feature selection process was embedded inside the LOCO training and testing iteration loops. In each LOCO training and testing process, one case was selected as an independent testing case and the remaining 150 cases were used as training cases. The WSE guided feature selection method was applied to all 150 training cases to search for optimal features from the entire feature pool and train an ANN based classifier. The trained ANN was then applied to one independent testing case and generates a classification score for the testing case (ranging from 0 to 1). The higher score indicates a higher probability of the tumor responding to the neoadjuvant chemotherapy or being classified into "CR" class. This LOCO process was repeated 151 times. As a result, 151 classification scores were independently generated for all 151 cases in our dataset. In the different LOCO training and testing iteration cycles, the potentially different image features may also be selected from the initial pool of features and used to build the ANN.

We then used the area under a receiver operating characteristic (ROC) curve (AUC), which was computed using a publically-available maximum likelihood based ROC curve fitting program (ROCKIT, http://www-radiology.uchicago.edu/krl/, University of Chicago), as an evaluation index to assess performance of the image features or ANN-generated classification scores associating with the tumor response to the neoadjuvant chemotherapy. The p-values were also computed by the ROCKIT program when any two sets of image feature data and/or ANN classification scores were used as input data of the ROCKIT program. All statistically significant differences were defined as the p-value smaller than 0.05. We compared the discriminatory power of using each individual features (as listed in Table 1) and the classification scores generated by the multi-feature based machine learning classifier (ANNs) using the LOCO validation method. In addition, we applied an operation threshold of 0.5, which is a middle point of the ANN-generated classification scores, and compute the overall classification accuracy as well as the predictive values of both "CR" and "PR" classes of our scheme in assessing the tumor response to the neoadjuvant chemotherapy.

III. RESULTS

When applying each of 10 individual image features computed in our initial feature pool (Table 2) to associate with or classify cases between the CR and PR groups, Table 3 shows and compares the computed AUC values. The AUC values ranged from 0.542±0.047 to 0.734±0.043. Among them, the average contrast enhancement value of entire breast volume or regions (*F1*) and standard deviation (*F2*) have the highest discriminatory power with AUC > 0.7.

Table 4 summarizes the percentage of each of 10 features selected during the 151 LOCO training and testing iteration cycles in building the ANN based classifier. Despite high AUC values of F2, it was not selected much during LOCO training and testing iteration cycles because of high correlation with other features (e.g., its correlation coefficient with *F1* is 0.984). The top 4 selected features that were selected ≥ 90% times in 151 LOCO cycles were average enhancement value of entire breast area (*F1*), average of bilateral enhancement value difference between left and right breasts (*F7*), standard deviation of bilateral enhancement value difference between left and right breast (*F8*) and average of bilateral enhancement value of top 5% difference between left and right breast (*F10*). This indicates that these 4 features played the most important interaction role in developing our ANN based classification model. Three of these features were computed from the bilateral asymmetry of the contrast enhancement features computed between the left and right breasts. Although using each individual image features may only have limited discriminatory power (or AUC values), developing a multiple feature ANN-based classifier enabled to yield a significantly higher assessment performance with AUC = 0.83±0.04 than using each feature individually ($p < 0.05$). Figure 3 shows and compares 5 ROC curves generated using the classification scores generated by the ANN-based classifier and each of four commonly selected image features.

As an example, Table 5 presents the computed feature values and ANN-generated classification scores of 3 example cases (as shown in Figure 1). CR case has the highest classification score. Except feature (*F10*) of case 3, the trend between ANN-generated classification scores and other feature values are also demonstrated. Table 6 shows a confusion matrix that was obtained by applying an operation threshold of 0.5 to the classification scores generated by the ANN-based classifier. The overall assessment accuracy to these two groups of 151 CR and PR cases was 82%, in which 124 cases were correctly classified into “CR” and “PR” classes, while the remaining 27 cases were incorrectly classified. The predictive values of “CR” and “PR” case group are 86.0% (43/50) and 80.2% (81/101), respectively.

IV. DISCUSSION

Since breast MRI is considered a very useful imaging modality in assessing breast tumor response to neoadjuvant chemotherapy (9, 10), developing and applying breast MRI image feature analysis based on the quantitative image feature analysis or CAD schemes to assess complete response of the breast tumors to the neoadjuvant chemotherapy has been attracting research interest (20, 21). In this paper we reported our latest progress to develop and test new quantitative image feature analysis schemes to assess breast tumor response to the neoadjuvant chemotherapy. This study has a number of unique characteristics. First, we tested the feasibility whether with the help of automated segmentation of breast region depicted on the breast MR images acquired before pre-chemotherapy, applying a new CAD scheme and machine learning classifier optimized using the quantitative global kinetic breast MR image features had potential to generate useful clinical image marker in assessing tumor response to neoadjuvant chemotherapy. Our study results support the hypothesis that the global background parenchymal enhancement (BPE) of breast MRI carries useful clinical information, which may be used to assess breast cancer risk (14), classify between malignant

and benign breast MRI examinations (15). In this study, we demonstrated that using BPE-related image features could also effectively assess tumor response to neoadjuvant chemotherapy.

Second, unlike many previously developed CAD schemes of breast MR images including our own scheme (13), which computed and use the kinetic image features only from the segmented tumor regions, CAD scheme developed in this study does not segment the targeted tumors from the breast MR images. As a result, the new CAD scheme is much simple and probably also more robust to be applied to the different breast MR images with diverse clinical patterns because the automated tumor segmentation process is not only often complicated but also difficult and/or not robust in particular for segmenting the diffusive tumors depicting on breast MR images. Although the maximum contrast enhancement typically occurs inside a malignant breast tumor as measured by feature *F4*, the study results showed that using *F4* did not yield highest classification performance as comparing several features computed from the global breast MR images including average contrast enhancement (*F1*) and standard deviation of the contrast enhancement (*F2*), which indicates that tumor response to the neoadjuvant chemotherapy depends more on the overall contrast enhancement patterns generated from both tumor and background parenchymal tissues.

Third, besides computing the global BPE features from the entire breast MR images, we also computed bilateral images feature asymmetry between left and right breasts. We observed that unlike in assessing breast cancer risk (22), the computed kinetic enhancement feature difference between two bilateral breast MR images is relatively bigger and classification performance of using such single feature is lower than using the global BPE features. However, these features are still very useful to build a highly performed multi-feature fusion based classifier. When embedding a wrapper subset evaluator inside a LOCO based cross-validation method to select optimal features and optimize the ANN classifier, three bilateral BPE kinetic feature asymmetry were among the four mostly selected image features. The results indicate that the applied machine learning method was effective, which enables to select and optimally fuse non-redundant image features and eliminate the redundant (or highly correlated) features (i.e., features *F1* and *F2*).

Fourth, this is a retrospective study. We applied our CAD scheme to a relatively diverse image database randomly collected from the existing clinical database. The dataset is relatively balanced in which there are no statistically significant differences in patients' age ($p = 0.445$) and solid tumor sizes ($p = 0.509$) between CR and PR patient groups. Hence, our study results support a recently emerged Radiomics concept that hypothesized that quantitative image features enabled to phenotype many useful biological or gene-expression process of cancer development and prognosis (23), which provides a simple approach to improve decision-making in cancer treatment at low cost (24).

There are also several limitations in this study. For example, (1) this is a laboratory based retrospective study using a relatively small data size (with 151 cases). Thus, the robustness of our study results needs to be further tested in future studies with large and diverse image datasets. (2) Due to our small dataset, our CAD scheme was only trained and applied to classify cases into CR and PR groups. (3) To make our CAD scheme simple, the scheme

does not involve a non-rigid image registration algorithm in attempt to register MR image slices acquired pre- and post-contrast enhancement scans. However, due to the lack of ground-truth, no accurate non-rigid image registration algorithm is available to date. This issue needs to be further developed and investigated. (4) This is a single institutional study. The guidelines of neoadjuvant chemotherapy for the breast cancer patients may vary at different medical institutions. Thus, whether our CAD scheme can be optimally applicable to the images acquired from other medical institutions also needs to be tested in future studies.

In conclusion, in this study we developed and tested a new CAD scheme based on the quantitative global kinetic breast MR image feature analysis. From our study we demonstrated the feasibility of identifying a new image feature based clinical marker to assess breast tumor response to the neoadjuvant chemotherapy. Our study results support the new concept of Radiomics (23, 24) in which the high association or supplementary information between the quantitative radiographic image features and genomic biomarkers can be found. As a result, although many genomic biomarkers have been performed in the effort to associate with breast tumor response to neoadjuvant chemotherapy, our study suggested that the quantitative image features computed from breast MR images also enabled to provide highly discriminatory information, which can be more easily extracted from the existing diagnostic breast MR images and yield high clinical impact and cost-effectiveness.

ACKNOWLEDGEMENT

This work is supported in part by Grants of R01 CA160205 and R01 CA197150 from the National Cancer Institute, National Institutes of Health. The authors would also like to acknowledge the support from the Peggy and Charles Stephenson Cancer Center, University of Oklahoma

VI. REFERENCES

1. Sardanelli F, Podo F. Breast MR imaging in women at high-risk of breast cancer. Is something changing in early breast cancer detection? Eur Radiol. 2007; 17:873–887. [PubMed: 17008989]
2. Berg WA, Zhang Z, Lehrer D, et al. Detection of breast cancer with addition of annual screening ultrasound or a single screening MRI to mammography in women with elevated breast cancer risk. JAMA. 2012; 307:1394–1404. [PubMed: 22474203]
3. Saslow D, Boetes C, Burke W. American Cancer Society guidelines for breast screening with MRI as an adjunct to mammography. CA Cancer J Clin. 2007; 57:75–89. [PubMed: 17392385]
4. Bhooshan N, Giger ML, Jansen SA, Li H, Lan L, Newstead GM. Cancerous breast lesions on dynamic contrast-enhanced MR images: Computerized characterication for image-based prognostic markers. Radiology. 2010; 254:680–690. [PubMed: 20123903]
5. Graham LJ, Shupe MP, Schneble EJ. Current approaches and challenges in monitoring treatment response in breast cancer. J Cancer. 2014; 5:58–68. [PubMed: 24396498]
6. Fisher B, Bryant J, Wolmark N. Effect of preoperative chemotherapy on the outcome of women with operable breast cancer. J Clin Oncol. 1998; 16:2672–2685. [PubMed: 9704717]
7. Van der Hage JA, Van de Velde CJ, Julien JP. Preoperative chemotherapy in primary operable breast cancer: results from the European Organization for Research and Treatment of Cancer Trial 10902. J Clin Oncol. 2001; 19(22):4224–4237. [PubMed: 11709566]
8. Mauri D, Pavlidis N, Ioannidis JP. Neoadjuvant versus adjuvant systemic treatment in breast cancer: a meta-analysis. J of the National Cancer Inst. 2005; 97(3):188–194.

9. Lobbes MB, Prevos R, Smidt M, Tian-Heijnen VC, et al. The role of magnetic resonance imaging in assessing residual disease and pathologic complete response in breast cancer patients receiving neoadjuvant chemotherapy: a systematic review. Insights Imaging. 2013; 4:163–175. [PubMed: 23359240]
10. Marinovich ML, Houssami N, Macaskill P, et al. Meta-analysis of magnetic resonance imaging in detecting residual breast cancer after neoadjuvant therapy. J Natl Cancer Inst. 2013; 105:321–333. [PubMed: 23297042]
11. Eisenhauer EA, Therasse P, Bogaerts J, et al. New response evaluation criteria in solid tumours: Revised RECIST guideline (version 1.1). Eur J Cancer. 2009; 45:228–247. [PubMed: 19097774]
12. Rouzier R, Perou CM, Symmans WF, et al. Breast cancer molecular subtypes respond differently to preoperative chemotherapy. Clin Cancer Res. 2005; 11:5678–5685. [PubMed: 16115903]
13. Aghaei F, Tan M, Hollingsworth AB, Qian W, Liu H, Zheng B. Computer-aided Breast MR Image Feature Analysis for Prediction of Tumor Response to Chemotherapy. Med Phys. 2015; 42:6520–6528. [PubMed: 26520742]
14. King V, Brooks JD, Bernstein J. Background parenchymal enhancement at breast MR imaging and breast cancer risk. Radiology. 2011; 260:50–60. [PubMed: 21493794]
15. Yang Q, Li L, Zhang J, Shao G, Zheng B. A computerized global MR image feature analysis scheme to assist diagnosis of breast cancer: a preliminary assessment. Eur J Radiol. 2014; 83:1086–1091. [PubMed: 24743001]
16. Chen W, Giger ML, Bick U, Newstead GM. Automatic identification and classification of characteristic kinetic curves of breast lesions on DCE-MRI, Med. Phys. 2006; 33:2878–2887.
17. Witten, I.; Frank, E.; Hall, MA. Data mining: practical machine learning tools and techniques. 3rd ed. Elsevier; http://www.cs.waikato.ac.nz/ml/weka/
18. Kohavi R, John GH. Wrappers for feature subset selection. Artificial Intelligence. 1997; 97:273–324.
19. Li Q, Doi K. Reduction of bias and variance of evaluation of computer-aided diagnostic schemes. Medical Physics. 2006; 33:868–875. [PubMed: 16696462]
20. Anger SC, Rosen MA, Englander S, et al. Computerized image analysis for identifying triple-negative breast cancers and differentiating them from other molecular subtypes of breast cancer on dynamic contrast-enhanced MR images: A feasibility study. Radiology. 2014; 272:91–99. [PubMed: 24620909]
21. Schacht DV, Drukker K, Pak I, Abe H, Giger ML. Using quantitative image analysis to classify axillary lymph nodes on breast MRI: a new application for the Z 0011 Era. Eur J Radiol. 2015; 84:392–397. [PubMed: 25547328]
22. Zheng B, Sumkin JH, Zuley ML, Wang X, Klym AH, Gur D. Bilateral mammographic density asymmetry and breast cancer risk: A preliminary assessment. European Journal of Radiology. 2012; 81:3222–3228. 2012. [PubMed: 22579527]
23. Lambin P, Rios-Velazquez E, Leijenaar R, et al. Radiomics: extracting more information from medical images using advanced feature analysis. Euro J Cancer. 2012; 48:441–446.
24. Aerts H, et al. Decoding tumor phenotype by noninvasive imaging using a quantitative Radiomics approach. Nat. Commun. 2014; 5 4006-1-8.

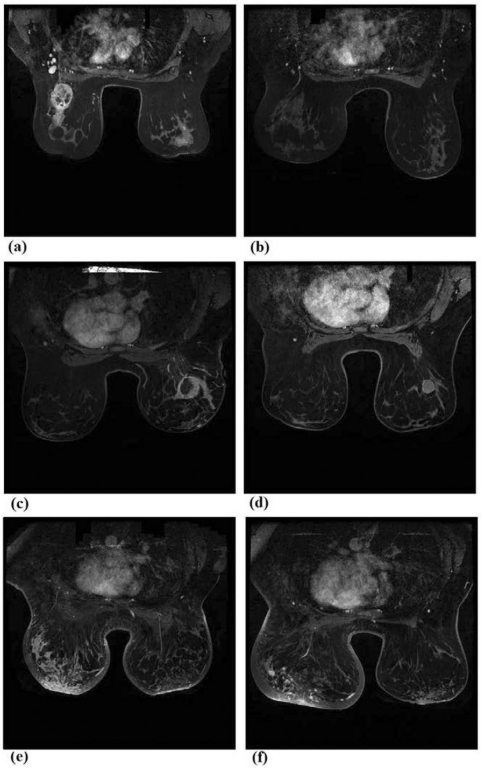

Figure 1.
Three examples of showing two matched breast MR image slides acquired from pre- and post-chemotherapy of one CR case (a) and (b), one PR case with solid contrast enhanced tumor (c) and (d), and one PR case with the diffused lesion enhancement (e) and (f).

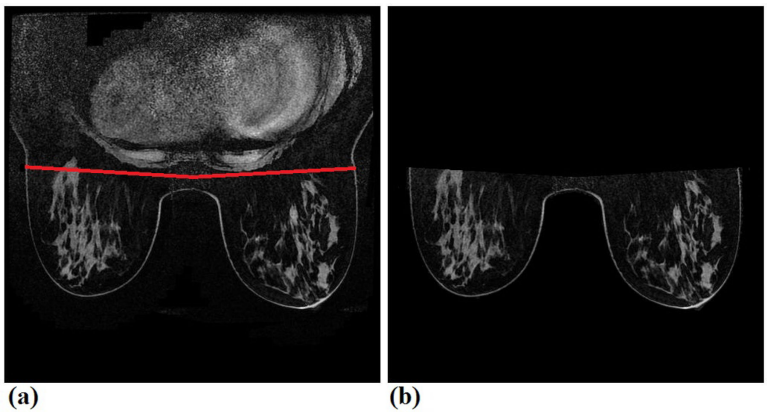

Figure 2.

An example to show chest wall detection and breast region segmentation, in which (a) shows an original image slice marked by two CAD scheme detected lines to segment between two breasts and chest regions, and (b) shows the final segmented breast regions, which are used to compute the BPE features.

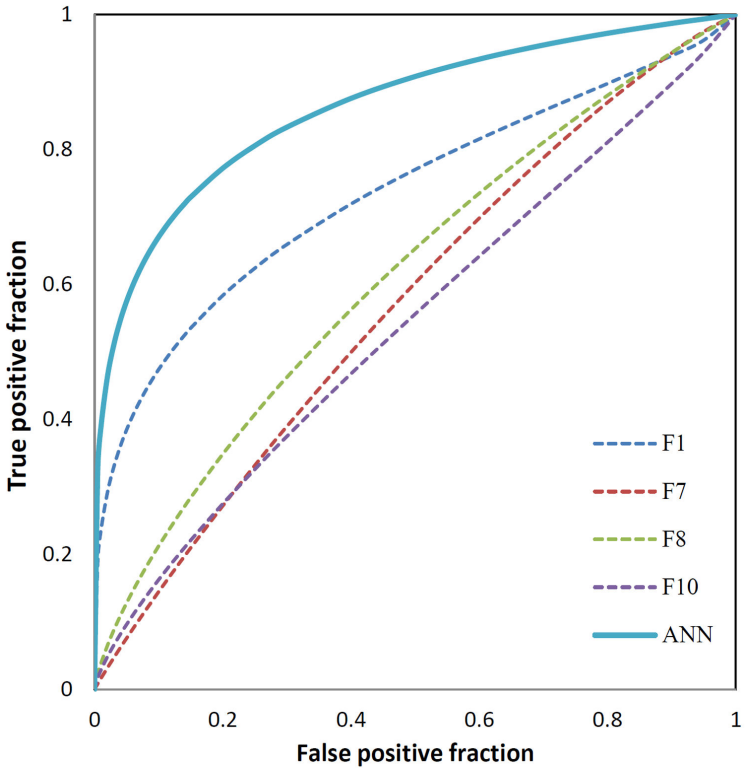

Figure 3.

Comparison of 5 ROC curves generated using the classification scores of the ANN-based classifier (solid curve) and other four individual features (dashed curve)

Table 1

Distribution of tumor subtypes in both CR and PR case groups

Tumor Characteristics	CR	PR
Number of solid tumors	25	43
Average size of solid tumors	29.48±10.41	31.69±15.62
Number of diffused tumors	38	45
Tumor pathology subtypes		
Invasive ductal carcinoma (IDC)	26	27
IDC and DCIS	28	45
Invasive lobular carcinoma (ILC)	2	1
ILC and DCIS	2	1
Infiltrating carcinoma	0	1
Invasive mammary carcinoma	0	3
Poorly differentiated carcinoma	5	10

Table 2

Description of 10 computed global kinetic image features.

Feature	Description	Feature	Description
F1	Average enhancement value (EV)	F6	Average EV of top 5%
F2	Standard deviation of EV	F7	Bilateral average EV difference
F3	Skewness of EV	F8	Bilateral STD EV difference
F4	Maximum EV	F9	Bilateral difference of average EV of top 1%
F5	Average EV of top 1%	F10	Bilateral difference of average EV of top 5%

Table 3

AUC values of applying 10 individual features (given in Table 1) to classify between CR and PR group of cases.

Feature	AUC	Feature	AUC
F1	0.734±0.043	F6	0.623±0.046
F2	0.723±0.043	F7	0.572±0.047
F3	0.695±0.508	F8	0.613±0.046
F4	0.581±0.047	F9	0.542±0.047
F5	0.596±0.047	F10	0.542±0.048

Table 4

A list of 10 image features that were selected in LOCO training and testing iteration cycles to test 151 testing cases in our dataset.

Feature	Percentage	Feature	Percentage
F1	100%(151/151)	F6	60%(91/151)
F2	36%(55/151)	F7	100%(151/151)
F3	0%(0/151)	F8	100%(151/151)
F4	11%(16/151)	F9	56%(85/151)
F5	62%(93/151)	F10	90%(139/151)

Table 5

Feature values of three cases with images shown in Figure 1.

Feature	Case 1 (up)	Case 2 (middle)	Case 3 (bottom)
F1	0.29	0.39	0.6
F7	0.32	0.66	1
F8	0.37	0.6	0.76
F10	0.48	0.83	0.42
ANN	0.996	0.254	0.045

Table 6

A confusion matrix of classification scores generated using an ANN-based classifier that was trained using 4 selected image features.

Prediction Result / Actual Cases	**CR**	**PR**
CR	43	20
PR	7	81